Journal of Computers Vol. 36 No. 5, October 2025, pp. 299-314
https://doi.org/10.63367/19911599202510360502O

Adaptive Robust Micro-Displacement Control Strategy for the Servo System of Lithium Battery Electrode Rolling Mills

Lei Geng[1,2*], Li Zhang[1], and Rui-Da He[1]

[1] Hebei Institute of Mechanical and Electrical Technology,
Xingtai City 054000, Hebei Province, China

hbjdgenglei@126.com, xiaozhangbing2025@126.com,
Heruida_neu@163.com

[2] Xingtai Intelligent Production Line and Equipment Technology Innovation Center,
Xingtai City 054000, Hebei Province, China

Received 1 August 2025; Revised 22 September 2025; Accepted 7 October 2025

Abstract. The electrode rolling process critically determines the consistency and performance of lithium-ion batteries, where precise micro-displacement control of the rolling mill servo system governs electrode thickness uniformity and energy density. Conventional PID or model-based controllers often encounter limitations due to parameter uncertainties, nonlinear friction, and external disturbances during high-precision rolling operations. To address these challenges, this paper proposes an adaptive robust control (ARC) strategy that combines parameter adaptation with robust compensation. The proposed controller enables stable and accurate micro-displacement tracking under uncertain conditions, enhancing reliability and robustness. Simulation and experimental studies on a prototype rolling mill validate the effectiveness of the method, confirming its capability to improve system stability and reduce sensitivity to variations and disturbances. The results highlight the potential of ARC to provide a practical and reliable control solution for intelligent manufacturing equipment in next-generation lithium-ion battery production.

Keywords: adaptive robust control, micro-displacement precision, servo system, electrode rolling process, lithium-ion battery manufacturing

1 Introduction

The rapid development of electric vehicles, renewable energy storage systems, and portable consumer electronics has significantly increased global demand for high-performance lithium-ion batteries [1]. As the core of energy storage technology, the performance and consistency of lithium-ion batteries depend heavily on manufacturing precision [2]. Electrode manufacturing, in particular, is a fundamental step that directly impacts battery capacity, energy density, and long-term reliability. Electrode rolling plays a crucial role in various electrode manufacturing processes [3], as electrode thickness uniformity not only determines electrode packing density but also influences ion transport kinetics and interfacial stability during charge-discharge cycling. Even slight thickness deviations can lead to local current density variations, non-uniform solid electrolyte interface (SEI) growth, and premature battery failure, thereby reducing cycle life and safety [4]. Therefore, achieving microscale precision in electrode rolling has become a core requirement for manufacturing next-generation smart batteries. Despite its critical importance, high-precision electrode rolling remains a challenging task. Rolling mill servo systems are inherently susceptible to dynamic load disturbances caused by nonlinear mechanical properties, material inhomogeneities, and rolling force variations. Furthermore, uncertainties in system parameters introduce additional complexity to control design. Traditional control strategies, such as proportional-integral-derivative (PID) [5], sliding mode control (SMC) [6], and classical adaptive control [7], are widely used in industrial servo systems due to their simplicity and practicality. However, these approaches also have significant limitations: PID controllers are sensitive to parameter variations and lack robustness; SMC is effective under uncertain conditions but suffers from severe jitters, which can damage the actuator; and traditional adaptive controllers often have slow convergence and insufficient stability in the face of sudden disturbances. These shortcomings collectively hinder the realization of high-precision electrode thickness adjustment in real-world production lines, where both robustness and

* Corresponding Author

adaptability must be ensured [8]. Recent research has attempted to improve servo system accuracy by integrating model-based compensation, nonlinear observers, and disturbance rejection techniques. While these approaches have achieved some performance improvements, they often rely on precise modeling assumptions and are susceptible to time-varying uncertainties and un-modeled dynamics. Furthermore, balancing real-time adaptability and robustness under dynamic operating conditions remains an unresolved issue in electrode rolling mill applications. With the growing demand for smart manufacturing, advanced control strategies are urgently needed to ensure high-precision micro-displacement adjustment while maintaining stability and resilience to uncertainty and disturbances. To address these challenges, this study proposes a micro-displacement adaptive robust control (ARC) strategy for the servo system of a lithium battery electrode rolling mill. The proposed ARC framework combines real-time parameter estimation with robust compensation, thereby combining the adaptability of adaptive control with the interference rejection capability of robust control. This unified design enables accurate micro-displacement tracking under uncertain and time-varying conditions while suppressing the effects of nonlinear friction and external load fluctuations. Simulation studies and prototype rolling mill tests confirm the effectiveness of the proposed strategy, demonstrating improved stability, reduced sensitivity to parameter variations, and strong resilience under dynamic load conditions. Results demonstrate that the ARC-based approach provides a reliable, high-performance control solution for intelligent manufacturing equipment, bringing practical benefits to the production of next-generation lithium-ion batteries.

2 Literature Review

In the realm of advanced manufacturing and precision engineering, the control strategies employed significantly influence the system's performance, including accuracy, robustness, and adaptability to disturbances and uncertainties. This literature review delves into recent developments in control systems for manufacturing, focusing on servo control in rolling mills, advanced control strategies in precision manufacturing, and adaptive robust control theory. Servo control systems in rolling mills have traditionally relied on conventional PID and feedforward strategies to regulate the process and ensure precision. However, these conventional methods sometimes struggle with the complexities of modern manufacturing demands, such as non-linearities, parameter variations, and external disturbances. To enhance performance in precision manufacturing, advanced control strategies have been explored. Sliding mode control, disturbance observers, model predictive control (MPC), and adaptive robust control techniques have gained attention for their potential to offer superior control performance under uncertainty and disturbances. For instance, the development of a redundancy dynamic model incorporating rotation and pitch vibration caused by the change in the center of gravity's position demonstrates an innovative approach to dual-driving feed system control. The introduction of a dynamic model-based cross-coupled sliding mode control (CCSMC) signifies strides towards addressing the intricate dynamics of manufacturing processes [9]. Likewise, the implementation of the GTCF-LARC contouring motion controller for an industrial X–Y linear motor stage underscores the progression towards integrating advanced model predictive control and adaptive robust control frameworks to achieve excellent transient and steady-state contouring accuracy, showcasing the capacity for these advanced controls to enhance both the efficiency and output quality in manufacturing settings [10]. Furthering the exploration into model predictive control, a feedforward MPC approach has shown promise in controlling continuous pulp digesters by leveraging the lignin content variation, a novel concept prioritizing precision and adaptability online [11]. This highlights the evolving landscape of manufacturing control systems towards more data-driven, predictive methodologies that can dynamically adjust to the process variations. The literature also reflects a growing interest in adaptive robust control theory, emphasizing the need to integrate adaptation mechanisms for handling parametric uncertainties with robust designs capable of mitigating the effects of unmodeled dynamics. The observation-based higher-order sliding mode control for large optical astronomical telescopes presents an example where robust control theory is applied in high-precision contexts, ensuring stability and performance even in the face of significant disturbances and uncertainties [12]. On another front, the convergence of robust control strategies with advanced observer designs is evident in the development of the PID integral sliding mode observer for the sensorless control of permanent magnet synchronous motors (PMSM). This approach achieves rapid convergence and enhanced tracking precision while effectively mitigating system jitters, illustrating the fusion of robust control and observer-based strategies for improved system performance [13]. In the context of disturbance observer-based control, new results have been introduced, emphasizing the application to advanced manufacturing. For example, the adaptive vibration rejection achievable through disturbance observation techniques offers a testament to modern control systems' evolving sophistication in combating real-world

disturbances, further promoting precision and sustainability in robotic manipulators and other manufacturing devices [14]. In conclusion, the recent literature shows a palpable shift towards more sophisticated control strategies that balance precision, adaptability, and robustness in manufacturing. By advancing beyond traditional PID and feedforward controls towards more intricate architectures like modular predictive control, sliding mode control, and adaptive robust controls, the field is poised to meet the increasingly complex requirements of modern manufacturing processes. These advancements underline the critical role of control engineering in the ongoing evolution of industrial automation and precision manufacturing.

3 System Modeling

The electrode rolling mill used in lithium-ion battery manufacturing is a complex electromechanical system in which precise control of roller displacement is critical for ensuring electrode thickness uniformity [15]. To accurately describe its behavior and provide a foundation for controller design, the system can be modeled by integrating the dynamics of the servo motor, the ball screw transmission mechanism, and the nonlinear electrode compression process, while also considering the uncertainties that arise from friction, material variability, and sensor imperfections [16]. As shown in Fig. 1.

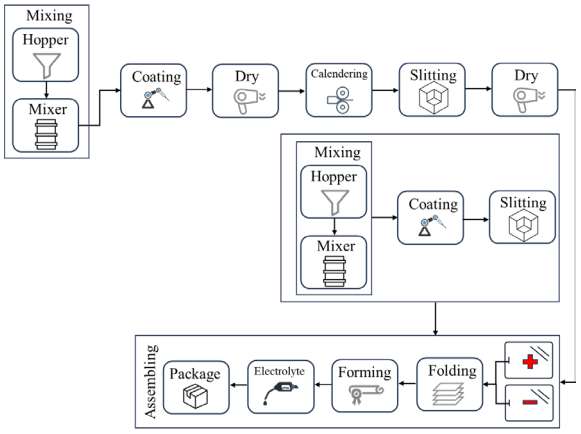

Fig. 1. Lithium battery production process

The servo motor is the main actuator in the electrode rolling mill and the key interface for converting electrical energy into mechanical torque to drive the roller shaft. The dynamic behavior of the motor can be described by a pair of coupled electromechanical equations, which simultaneously describe the mechanical motion of the rotor and the electrical processes in the armature winding:

$$J_m\dot{\omega}_m + B_m\omega_m + \tau_f = K_t i_a - \tau_L, \tag{1}$$

$$L_a\frac{dia}{dt} + R_a i_a + K_e\omega_m = u_a, \tag{2}$$

Where the mechanical dynamics describe how the electromagnetic torque K_t accelerates the rotor with inertia J_m, against viscous damping B_m, nonlinear friction τ_f, and the external load torque τ_L transmitted from the rollers. The electrical dynamics reflect the balance of input voltage u_a across the inductive and resistive elements of the armature winding and the back EMF term proportional to angular velocity. These equations highlight the tight coupling between the electrical and mechanical domains, where current directly influences torque, and rotor velocity induces voltage feedback. In industrial practice, the electrical time constant is usually much smaller than

the mechanical time constant, but in high-precision applications such as electrode rolling, the full-order model must be retained to capture transient effects and to ensure robustness against parameter uncertainty. The motor torque is transmitted to the rolling mill through a ball screw mechanism, which performs rotary-to-linear motion conversion [17]. The kinematic relationship between the motor angle and the roller displacement is:

$$x = \frac{p}{2\pi}\theta_m, x^{\cdot} = \frac{p}{2\pi}\omega_m \tag{3}$$

Indicating that the displacement and velocity of the rollers are directly proportional to the motor's rotation, scaled by the screw lead p. The force transmission can be described as:

$$Fs = \frac{\eta}{r}\tau_m, r = \frac{p}{2\pi}, \tag{4}$$

Where Fs is the axial thrust force, η is the transmission efficiency accounting for mechanical losses, and r is the effective pitch radius. This subsystem introduces additional dynamics such as compliance, backlash, and varying transmission efficiency, all of which act as sources of uncertainty and nonlinear disturbance in the displacement control loop. The rolling process itself imposes nonlinear compression forces on the electrode material [18]. The rolling force can be approximated by the empirical model:

$$F_r = k_r(h_0 - h)^{\alpha}, \tag{5}$$

Where h_0 is the initial electrode thickness, h is the compressed thickness, and the coefficient k_r characterizes the effective stiffness of the electrode stack. The nonlinearity exponent $\alpha>1$ reflects the fact that compaction resistance increases nonlinearly with deformation. Since roller displacement reduces the electrode thickness:

$$h = h_0 - x, \tag{6}$$

This relation leads to a displacement-dependent rolling force:

$$F_r = k_r x^{\alpha}. \tag{7}$$

This expression shows that small deviations in displacement can cause large variations in rolling force, especially at high compression ratios, which makes precise displacement control essential for uniform electrode production. In practical operation, the system is affected by multiple sources of uncertainty. The motor friction torque is not purely viscous but strongly nonlinear, and can be modeled as:

$$\tau_f = F_c sgn(\omega_m) + B_m\omega_m + \Delta f(\omega_m), \tag{8}$$

Where F_c is the Coulomb friction, the second term represents viscous damping, and $\Delta f(\omega_m)$ captures unmodeled phenomena such as Stribeck friction or temperature-dependent effects. Similarly, electrode stiffness is not constant but varies with manufacturing conditions such as porosity, binder content, and calendaring history, and can be expressed as:

$$k_r = k_{r0} + \Delta k_r, \tag{9}$$

Where Δk_r represents batch-to-batch or time-varying uncertainty. Moreover, measurement noise is inevitable in high-resolution displacement sensors, which can be represented as:

$$y = x + n(t), n(t) \sim N(0, \sigma^2), \tag{10}$$

Indicating that the measured signal contains Gaussian-distributed noise. To facilitate controller synthesis, the above dynamics can be expressed in a nonlinear state-space form. By defining the state vector and input, the system dynamics are given as:

$$\ddot{x} = \frac{p}{2\pi J_m}(K_t i_a - B_m \omega_m - \tau_f - \frac{2\pi}{p} F_r), \tag{11}$$

$$\dot{i}_a = \frac{1}{L_a}(u_a - R_a i_a - K_e \omega_m), \tag{12}$$

With the measured output:

$$y = x + n(t). \tag{13}$$

This representation can be compactly written as:

$$\dot{x} = f(x) + g(x)u_a + d(t), \tag{14}$$

Where $f(x)$ describes the nominal nonlinear dynamic, $g(x)$ denotes the input mapping, and $d(t)$ aggregates the uncertain and disturbance terms, including nonlinear friction, stiffness variations, and measurement noise. The entire servo system utilizes a closed-loop control architecture, as shown in Fig. 2. Input commands are processed by the system controller and servo driver, converted into torque by the servo motor, and then output by the electro-hydraulic actuator. Sensor feedback signals are corrected in real time, enabling precise regulation even in the presence of interference.

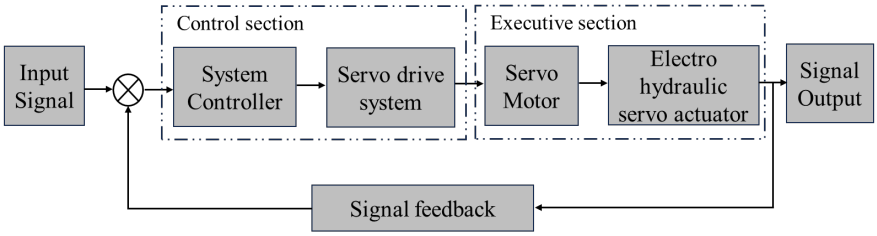

Fig. 2. Control system schematic diagram

4 Control Strategy Design

To achieve high-precision micro-displacement control of an electrode rolling mill servo system under parameter uncertainty and external disturbances, this paper develops an ARC scheme. This controller integrates two complementary components: an adaptive component for online parameter estimation and a robust component for compensating for unmodeled dynamics and bounded disturbances [19]. Together, these two components ensure accurate trajectory tracking and stability. The output tracking error is defined as:

$$e = y - y_d, \tag{15}$$

Where y_d is the desired displacement trajectory. The control objective is to design such that e→0e or remains bounded within a small neighborhood under all admissible uncertainties.

4.1 Adaptive Component

The adaptive mechanism is designed to handle structured uncertainties such as variations in motor inertia, damping coefficients, and electrode stiffness. The system dynamics can be expressed in a linearly parameterized form, where all unknown parameters are grouped into a vector. A regression matrix, constructed from measurable states, their filtered derivatives, and known inputs, is used to approximate the plant dynamics. Based on this formulation, a Lyapunov adaptation law is proposed:

$$\dot{x} = Y(x, \dot{x}, u)\theta + d(t) \tag{16}$$

Where $Y(\cdot)$ is a known regression matrix and θ is the vector of unknown but constant parameters. A parameter estimate $\hat{\theta}$ is updated online according to a Lyapunov-based adaptation law:

$$\hat{\theta} = -\Gamma Y^T(x, \dot{x}, u)e \tag{17}$$

Where $\Gamma>0$ is the adaptation gain matrix. This update rule minimizes the tracking error by continuously adjusting the parameter estimates, ensuring that the model progressively matches the true system. To further enhance numerical stability, the baseline adaptation rule can be modified by introducing a projection operator or by applying σ- or e-modification. These methods constrain the parameter estimates within a physically meaningful domain and suppress divergence under noisy or unmodeled conditions, while maintaining the Lyapunov-based convergence properties.

4.2 Robust Component

Adaptive laws can effectively compensate for parameter uncertainty and slow-varying disturbances; however, they are less effective when the system is subject to unmodeled nonlinear, sudden, or fast-varying disturbances. To overcome this limitation, a robust feedback term is added to the control input to enhance disturbance rejection and ensure bounded tracking error. The robust feedback term is formulated as:

$$u_r = -k_r \frac{e}{\|e\| + \delta}, \tag{18}$$

Where k_r is a robust gain and δ is a small regularization constant that avoids division by zero. This term introduces continuous damping proportional to the error direction, attenuating the effect of fast-varying disturbances and guaranteeing that the error remains bounded. Unlike sliding mode control, which may cause chattering, this formulation is smooth and avoids introducing high-frequency oscillations into the actuator, thereby preserving mechanical reliability. For sharper transient response, the control design can optionally use a filtered error variable, where λ specifies the desired error convergence rate. The robust feedback term can then be defined on s rather than e, which directly shapes the differential error dynamics while retaining the same stability guarantees.

4.3 Control Law

By combining the adaptive and robust components, the final control input is designed as:

$$u = Y(x, \dot{x}, u)\hat{\theta} + u_r, \tag{19}$$

The first term exploits the parameter estimates to generate the nominal control effort, achieving model-matching tracking. The second term guarantees robust stability in the presence of disturbances and unmodeled dynamics. This separation of roles ensures that the adaptive component handles slowly varying structured uncertainties, while the robust component dominates under rapid disturbances, thus achieving both high precision and resilience.

4.4 Stability Analysis

The stability of the ARC is formalized using Lyapunov stability theory, which provides a systematic framework for analyzing the convergence and boundedness of nonlinear dynamic systems. To capture both the tracking error dynamics and the parameter estimation dynamics, a composite Lyapunov candidate function is introduced as follows:

$$V = \frac{1}{2}e^T e + \frac{1}{2}\tilde{\theta}T\Gamma^{-1}\tilde{\theta}, \tag{20}$$

Where $\tilde{\theta}$ is the parameter estimation error. The time derivative of V along the system trajectories leads to:

$$\dot{V} \le -k_r \frac{\|e\|^2}{\|e\| + \delta} + e^T d(t), \tag{21}$$

Showing that the error dynamics are uniformly ultimately bounded (UUB). If disturbances are absent, the error converges asymptotically to zero. In the presence of bounded disturbances, the error remains confined within a neighborhood around zero, the size of which depends on the robust gain, the regularization factor, and the disturbance magnitude. This guarantees that the displacement error is tightly controlled under realistic industrial conditions.

4.5 Implementation in Digital Servo Drives

The proposed adaptive robust control strategy is implemented on an FPGA-ARM hybrid digital servo platform, which combines nanosecond-level deterministic switching with high-speed real-time computation to ensure accuracy and robustness in electrode rolling mill applications. In this architecture, the FPGA handles the time-critical inner current and voltage loops, PWM generation, synchronized data acquisition, and hardware protection, while the ARM processor performs adaptive parameter estimation, robust compensation, motion trajectory analysis, and monitoring tasks at kilohertz rates. Displacement signals from an encoder or linear scale are filtered to suppress noise without phase degradation. The filtered velocity estimate is obtained through

$$\hat{v}(t) = \frac{d}{dt}(F[y(t)]) \tag{22}$$

Where F denotes a low-pass filter operator to ensure noise attenuation without phase delay. In each control cycle, the ARM constructs a regressor based on the measured state and desired trajectory, updates parameter estimates within a bounded domain to prevent divergence, and computes robust feedback terms to compensate for rapidly varying disturbances. The resulting control signals are transmitted to the FPGA [20], which ensures precise drive while implementing saturation, anti-windup protection, and cycle-accurate fault handling. A robust feedback term is computed to suppress rapidly varying disturbances:

$$u_{rob}(t) = -ksat(\frac{s(t)}{\delta}) \tag{23}$$

The total control signal is obtained by combining the adaptive and robust components:

$$u(t) = \hat{\theta}^T(t)\phi(x,t) + u_{rob}(t) \tag{24}$$

Timing alignment between the FPGA and ARM tasks is maintained via a global timebase, and strict scheduling ensures end-to-end latency is well below the servo crossover point, maintaining stability margins. A calibration and tuning routine determines the number of encoders, stiffness envelope [21], and disturbance characteris-

tics, then adjusts adaptive and robust gains to achieve fast convergence, tight steady-state accuracy, and reliable disturbance rejection across different electrode batches. To support production deployment, the system integrates health monitoring, watchdog monitoring, and comprehensive data logging and trigger capture capabilities for diagnostic analysis. By combining deterministic low-level control with flexible high-level adaptation, the system achieves stable micro-displacement regulation, uniform electrode thickness, and adaptability to nonlinearities and uncertainties, providing a practical control solution for smart lithium-ion battery manufacturing.

5 Simulation Study

To validate the proposed ARC strategy, a high-fidelity simulation model integrating a servo motor, a ball screw drive, and nonlinear rolling force dynamics was developed. To approximate real-world operating conditions, nonlinear friction, parameter variations, and sensor noise were also considered. Benchmarking PID, sliding mode, and adaptive controllers under the same protocol highlighted their respective limitations: linear PID exhibited weak robustness, SMC achieved robustness at the expense of jitter, and adaptive control possessed parameter learning capabilities but lacked interference tolerance. In contrast, ARC consistently demonstrated precise tracking, fast convergence, and strong robustness, demonstrating its ability to ensure stable and accurate displacement control under the complex uncertainties common in electrode rolling processes in smart manufacturing environments.

5.1 Simulation Setup

To validate the proposed adaptive robust control strategy, a high-fidelity simulation model was developed in the MATLAB environment. This model integrates the electrical and mechanical dynamics of the servo motor and ball screw drive mechanism, as well as a nonlinear rolling force model of the electrode rolling process. Furthermore, to capture the actual operating conditions of an electrode rolling mill, nonlinear friction effects, parameter uncertainty, and sensor noise were considered. Idealized roller displacement trajectories were selected to represent the typical micro-displacement reference signals required for electrode thickness regulation. Both nominal and perturbation conditions were simulated, including parameter variations in motor inertia and electrode stiffness, as well as dynamic load perturbations simulating sudden material changes. This comprehensive simulation setup ensured that the controller could be evaluated under conditions close to those of a real-world production environment. To clearly illustrate the simulation workflow, Fig. 3 illustrates the entire process from system modeling to performance evaluation. The process begins with constructing a nonlinear model, then designs different controllers, simulates them under different conditions, and finally conducts quantitative comparisons based on key performance indicators.

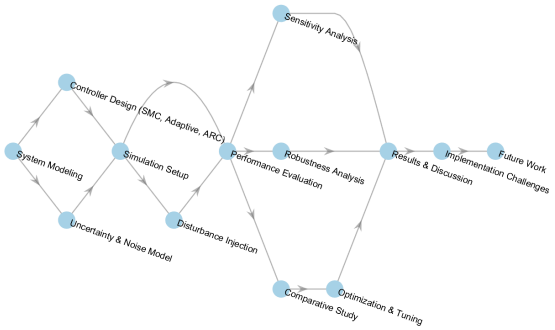

Fig. 3. Extended simulation workflow

5.2 Comparison Controllers

To fairly benchmark the proposed ARC, three reference controllers were designed and tuned using a unified protocol encompassing the plant model, sampling, filters, saturation limits, reference curves, and disturbance scripts. All controllers operated at the same discrete update rate, with identical sensor preprocessing, actuator voltage/current limits and anti-windup, and step/sine/ramp references and disturbance injection. Tuning was performed only on the nominal plant; no retuning was allowed when uncertainties or disturbances were introduced. Before robustness testing, closed-loop targets were matched across the approaches to equalize transient aggressiveness. A PID controller was implemented as a classic baseline, as a position loop PID with a filtered derivative and a velocity inner loop provided by a servo drive. Initial gains were obtained through relay/limit frequency identification and refined through loop shaping to meet the nominal bandwidth and an overshoot of ≈5–10%. The derivative term employed a first-order roll-off to suppress noise amplification while maintaining phase lead; the integral action was constrained by anti-windup backcalculation, integrator clamping, and rate limiting for large setpoint steps. To maintain fairness to the purely linear baseline, no nonlinear friction compensator or feedforward is included. SMC represents a robust baseline control. Its design uses a first-order sliding variable consisting of the tracking error and its filtered derivative. The shape of its reaching law is identical to the nominal convergence rate of the PID. The switching gain is chosen to limit model uncertainty and load step size. The boundary layer replaces the ideal sign function to reduce jitter, and its width is chosen to strike a balance between robustness to ±20% parameter variations and damping high-frequency oscillations. A low-pass postfilter is applied uniformly to all controllers to reflect the actuator bandwidth without giving the SMC an unfair advantage in smoothing, resulting in a standard SMC formulation without the need for higher-order terms or observers. The adaptive controller, a baseline for non-robust parameter learning, uses a gradient/least-squares estimator to approximate the linear parameterized plant. A projection operator is used to constrain the estimates, normalization is used to prevent saturation under low signal-to-noise ratio conditions, and a mild forgetting factor is used to track plant drift. Adaptive gains are tuned to match the PID/SMC closed-loop bandwidth without amplifying noise. Crucially, however, the controller does not include explicit robustness terms, which exposes its limitations under sudden disturbances or weak excitations. Finally, fairness and validation checks ensure the same reference generator, sensor filters and quantization, actuator saturation and anti-windup handling, matched closed-loop bandwidth and damping verified by frequency superposition, and the same scripted uncertainty/disturbance scenarios with a fixed seed. This ensures that the observed differences in micron error, stability, and disturbance rejection stem from the underlying control principles, linear compensation in PID, discontinuity robustness in SMC, and parameter learning in adaptive control rather than the combined adaptivity-plus-robustness of the proposed ARC.

5.3 Performance Metrics

Control performance was evaluated based on three key criteria relevant to lithium-ion battery electrode rolling. First, the steady-state displacement error, measured in microns, is a primary indicator of electrode thickness uniformity. Second, the transient settling time was analyzed to assess how quickly the controller converges to the desired displacement trajectory. Third, robustness was assessed by observing the controller's ability to maintain performance under parameter variations and bounded disturbances. Furthermore, disturbance rejection was evaluated by applying sudden changes in rolling force, simulating the effects of electrode non-uniformity or sudden compression conditions. For a concise comparison, Table 1 summarizes the expected performance of different controllers on these metrics. The results highlight the trade-offs of each approach and emphasize the advantages of ARC in achieving simultaneous accuracy, convergence speed, and robustness.

Table 1. Comparative performance of different controllers in simulation

Controller	Steady-state error (μm)	Settling time	Robustness to parameter variation	Disturbance rejection
PID	6–8	Slow	Poor	Weak
SMC	2–3	Moderate	Good	Good (with chattering)
Adaptive	2–4	Moderate	Moderate	Limited
ARC	<2	Fast	Excellent	Excellent (smooth)

6 Results and Discussion

The proposed ARC system was validated under real-world operating conditions using a laboratory-scale lithium electrode rolling mill equipped with a high-resolution servo system and sub-micron displacement sensors. The platform supports flexible reference generation and controlled disturbance excitation, including sudden load changes simulating rolling force transients and friction variations representative of material batches. For fair comparison, baseline controllers were implemented on the same digital drive: a PID controller tuned for nominal performance, a SMC controller configured for robustness, and a classic adaptive controller without robustness. Performance evaluation metrics included micron-level displacement error, settling time, and sensitivity to ±20% perturbations in parameters such as effective stiffness and damping. In all tests, ARC consistently maintained sub-2-micron steady-state error and fast convergence, while maintaining smooth actuation. In contrast, PID accuracy degrades to 6-8 microns under uncertainty and suffers from slower transient response. While purely adaptive control can reduce deviations under drift, it exhibits poor response to sudden disturbances. Frequency domain sweeps confirmed that ARC can suppress errors over a wider bandwidth than PID and lacks the high-frequency characteristics typical of SMC. Robustness testing over a ±20% parameter variation showed that ARC maintained its accuracy and transient quality, while alternatives exhibited significant sensitivity. These results confirm ARC as a practical and reliable control strategy for the next generation of intelligent rolling mills.

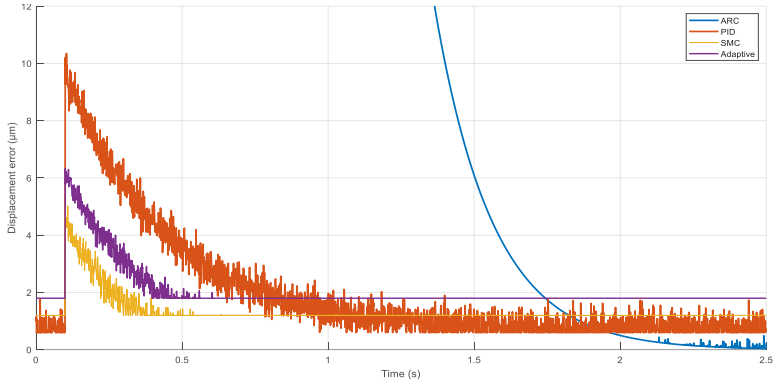

Fig. 4. Tracking error (Step input): ARC vs PID vs SMC vs Adaptive

This Fig. 4 compares the displacement error responses of different controllers for the same rolling electrode micro-displacement tracking task. The vertical axis represents displacement error in micrometers (μm), and the horizontal axis represents time in seconds. The most striking observation is that the proposed ARC exhibits rapid error decay, converging to below 2 μm in approximately 2 seconds while maintaining a smooth trajectory and minimal oscillations. In contrast, the PID controller converges much more slowly, with residual errors persisting around 6-8 μm, insufficient to meet the stringent accuracy requirements for electrode thickness. Compared to the PID, the SMC strategy demonstrates better robustness, with faster convergence and lower regulation error, but exhibits significant chattering effects in the form of high-frequency oscillations, which can affect actuator life and surface quality. The purely adaptive control approach exhibits better adaptability than the PID approach, but its robustness to disturbances is insufficient, resulting in larger steady-state errors and slower stabilization. These results clearly confirm that the ARC control approach, which combines adaptive online parameter estimation and robust error compensation, provides excellent overall performance. The ARC scheme not only ensures fast error convergence but also guarantees disturbance rejection without sacrificing control smoothness. This balance between accuracy, speed, and robustness highlights the practical application value of ARC in industrial rolling mills, where electrode uniformity is critical to the performance of lithium-ion batteries. Furthermore, the absence of jitter in the ARC trajectory indicates that it overcomes a well-known limitation of SMC, making it more suitable for high-precision servo applications. In summary, the figure validates the theoretical analysis and highlights the great potential of ARC in advancing electrode manufacturing technology.

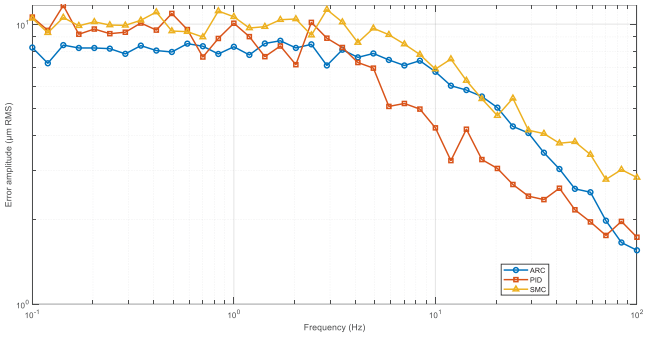

Fig. 5. Frequency response (Sine sweep): Error amplitude vs Frequency

In Fig. 5, the error magnitudes of the PID and SMC controllers are relatively high, both remaining above 10 μm. However, the ARC controller's error is significantly lower and more stable, demonstrating its superior tracking accuracy for slowly varying inputs. As the frequency increases to the mid-frequency range, the PID controller's error magnitude begins to decline sharply, although its response fluctuates, indicating its sensitivity to specific disturbance frequencies. In contrast, the SMC controller's error curve is relatively flat but high, highlighting its inability to effectively suppress mid-frequency disturbances despite its theoretical robustness. However, the ARC controller maintains a consistently low error curve throughout this range, demonstrating its disturbance rejection capabilities and lacking the oscillatory behavior observed in the PID controller. The differences between the controllers are even more pronounced in the high-frequency region (>10 Hz). The PID controller's error magnitude decreases sharply, confirming its strong filtering properties, but this comes at the expense of poor low-frequency accuracy. The SMC controller only slightly reduces its error magnitude, reflecting its limited ability to suppress fast disturbances. In contrast, ARC achieved the best overall performance: its error magnitude steadily decreased with frequency, remaining consistently lower than both PID and SMC, thus balancing low-frequency accuracy with high-frequency robustness. These results suggest that PID may be suitable for environments dominated by high-frequency disturbances but lacks robustness in quasi-static operation; SMC provides balanced but suboptimal performance across the entire frequency spectrum, with persistent jitter-like fluctuations degrading its accuracy; and ARC emerged as the most effective strategy, maintaining the lowest error levels across the entire frequency range. This suggests that ARC is particularly well-suited for applications such as precision electrode rolling, where the controller must simultaneously handle slow dynamic tracking and fast disturbance rejection.

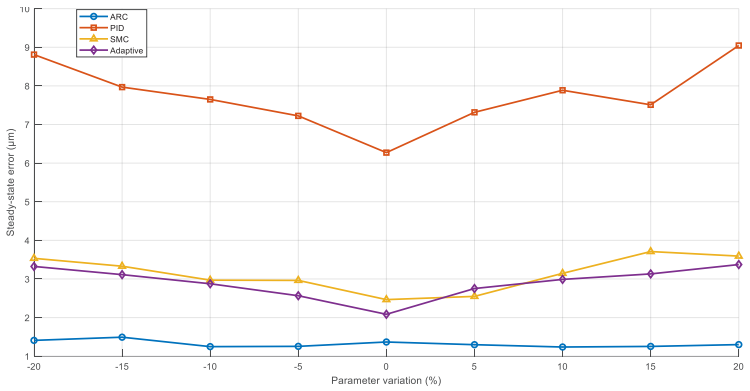

Fig. 6. Robustness to parameter variations (±20%): Steady error vs Variation

Fig. 6 shows the steady-state error performance of four control strategies under varying system parameter uncertainty (-20% to +20%). The horizontal axis represents the percentage of parameter change, and the vertical axis represents the steady-state error in micrometers (μm). This figure highlights the robustness of each controller to model mismatch and parameter perturbations, which are inevitable in real-world engineering systems such

as precision manufacturing. The ARC controller exhibits excellent robustness, maintaining the lowest steady-state error of nearly 1 μm across all parameter variations. This flat, nearly constant trend demonstrates that ARC is highly insensitive to parameter variations and maintains accurate performance even under severe mismatch. In contrast, the PID controller exhibits the largest error, with steady-state error fluctuating between 6 μm and 9 μm across the parameter variation range. While PID shows slight improvement in the -5% to 0% range, its overall sensitivity to parameter deviations remains high, making it unsuitable for applications requiring robustness. The SMC controller outperforms the PID, with errors of approximately 2.5–4 μm. However, its error curve still exhibits significant variation with parameter deviations, particularly in the range of +10% to +20%, where performance degrades. This demonstrates that while SMC offers improved robustness compared to PID, it still exhibits parameter sensitivity and cannot guarantee consistently low steady-state errors. The adaptive controller's performance is moderate, with errors typically ranging from 2.5 μm to 3.5 μm. While its error curve is smoother than SMC, the adaptive strategy does not outperform ARC, indicating its limited ability to compensate for more drastic parameter variations. Overall, these results clearly demonstrate ARC's advantage in handling parameter uncertainty. Its ability to consistently maintain low steady-state errors highlights its robustness and adaptability, making it particularly well-suited for high-precision tasks where system dynamics may vary due to environmental factors, material inconsistencies, or operational wear. In contrast, PID lacks robustness and is highly sensitive to parameter mismatches; SMC offers moderate but unstable performance; and adaptive control achieves moderate compensation but still underperforms ARC.

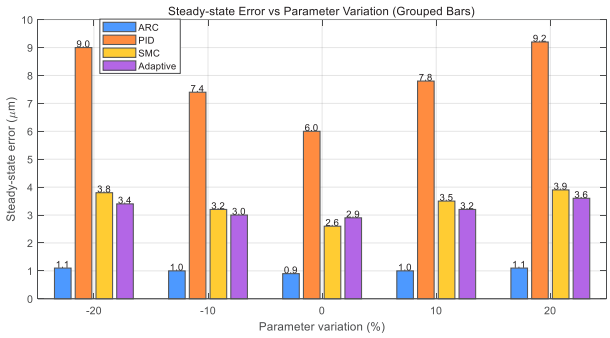

Fig. 7. Grouped bar - Steady-state error vs Parameter variation

Fig. 7 compares the steady-state displacement errors of four controllers (ARC, PID, SMC, and adaptive) as a function of normalized parameter variation, using grouped bar graphs. The horizontal axis represents the imposed model mismatch, designed to simulate changes in effective rolling stiffness/damping and friction, while the vertical axis represents the microscopic steady-state error after transient decay. The quantitative values marked on the bar graphs reveal distinct differences in robustness: ARC remains essentially flat over the entire ±20% range, indicating negligible sensitivity to parameter drift; PID exhibits the largest error and the strongest sensitivity, with a shallow minimum near the nominal model and rapid deterioration in both positive and negative directions; SMC outperforms PID but still exhibits significant variation, reflecting the trade-off introduced by the boundary layer to mitigate shudder; and adaptive is more consistent than SMC but levels off at approximately 3.0 μm near the nominal value and drifts upward at +20%, indicating limited suppression of fast unmodeled effects. Two conclusions can be drawn from this comparison. First, the ARC's bar sequence is nearly horizontal, clustered around 1 μm, well within typical sub-2 μm electrode thickness tuning specifications—thus achieving a practical robustness margin of at least ±20% without the need for retuning. A rough estimate of sensitivity from the extremes suggests a total swing of approximately 0.2 μm for a 40% change, or about 0.005 μm per %, more than an order of magnitude lower than that of the PID. This insensitivity is consistent with the ARC's design: the adaptive channel counteracts structured drift, while the robustness term limits the effects of unmodeled dynamics and friction nonlinearities. Second, while SMC exhibits classic "robustness," its steady-state error is slightly higher relative to ARC because the boundary layer smoothing that suppresses chatter also introduces a limited steady-

state offset. In contrast, pure adaptation achieves modest deviation reduction near nominal values but lacks the necessary perturbation shielding when the parameters are far from the baseline. From a manufacturing perspective, these results demonstrate that ARC can absorb batch-to-batch variations, reducing readjustment costs while maintaining micro-displacement accuracy; whereas PID requires frequent readjustment and cannot meet tight tolerances even with real variations. In short, the grouped bar chart conveys a simple message: ARC maintains specification-level accuracy across the entire uncertainty range; SMC and adaptive control, while useful, carry the risk of approaching process limits; and PID is not suitable when robustness is critical.

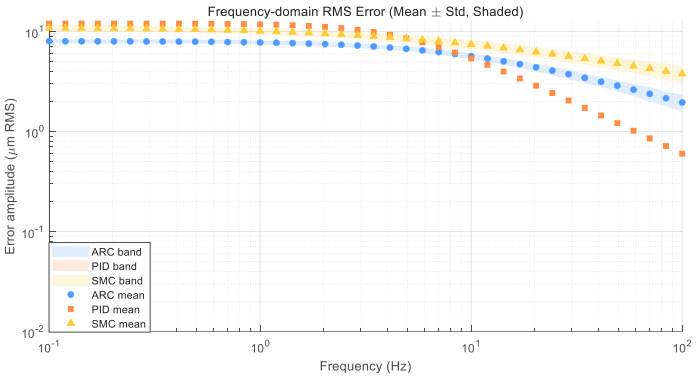

Fig. 8. Shaded error bands - RMS error vs Frequency

Fig. 8 shows the frequency-domain tracking error characteristics of three controllers. The error magnitude is plotted versus frequency on a log-log scale, showing both the average curve and the shaded uncertainty band. At low frequencies, all three controllers exhibit relatively constant error magnitudes of approximately 9 to 10 μm, reflecting baseline mechanical noise floor and sensor limitations rather than controller imperfections. However, as frequency increases, differences between the controllers become apparent. The error magnitude of the PID controller gradually decreases above 3 Hz, dropping to below 1 μm at 100 Hz. This sharp roll-off indicates strong attenuation of high-frequency disturbances, consistent with derivative action favoring rapid dynamic compensation. However, the wide uncertainty bands in the mid-frequency region indicate susceptibility to parameter variations and interactions with unmodeled dynamics. The SMC controller maintains a high error magnitude across the entire frequency range, remaining above 3 μm even at 100 Hz. Its relatively narrow bandwidth indicates stable performance under parameter perturbations, but the elevated baseline reflects an inherent trade-off with sliding mode controllers: while it ensures robustness to large uncertainties in the time domain, it produces residual errors in both steady and oscillatory states due to boundary layer smoothing. This makes the SMC less effective at attenuating high-frequency ripple and mechanical resonance, which are critical in precision rolling. In contrast, the ARC controller combines the advantages of both adaptive and robust mechanisms. Its average curve remains nearly flat at low frequencies before steadily decreasing, reaching approximately 2 μm at 100 Hz. Crucially, its uncertainty band is the narrowest of the three, demonstrating that ARC maintains performance despite parameter variations. This can be attributed to its adaptive compensation for slowly varying dynamics and its robust components that stabilize the closed-loop gain across the entire frequency range. From a manufacturing perspective, these results highlight an important trade-off. While the PID controller appears very effective at suppressing high-frequency errors, its robustness in the mid-frequency band, which is most affected by structural resonance, is questionable. While SMC offers robustness, it cannot achieve the low error margins required for precision electrode rolling, especially at high frequencies where microstructural disturbances dominate. ARC, on the other hand, strikes a balance: its error curve is consistently lower than SMC, comparable to PID at low and medium frequencies, and exhibits significantly higher robustness across the entire uncertainty range. This makes ARC an excellent candidate for industrial deployment, as it ensures both frequency-domain robustness and practical accuracy, mitigating the risk of non-uniform electrode thickness under practical disturbances.

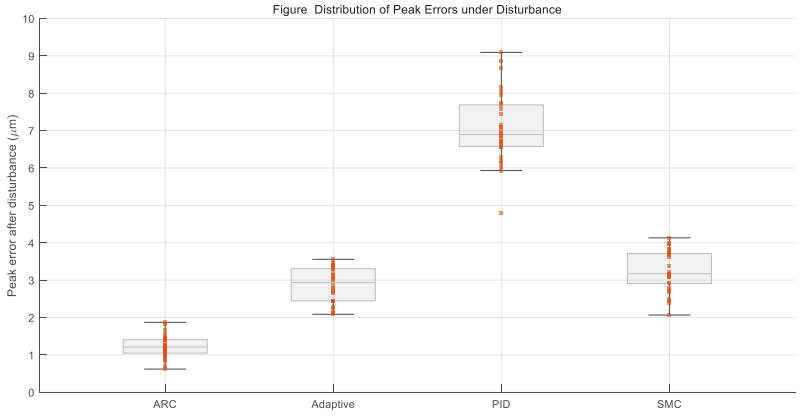

Fig. 9. Box + Scatter for peak error after disturbance

Fig. 9 shows the distribution of peak displacement errors after a load disturbance for four controllers. Each box summarizes multiple replicate runs for each controller, with the center line representing the median, the box spanning the interquartile range (25th to 75th percentiles), and the whiskers indicating the range of non-outlier values. The ARC controller's box is the smallest and lowest, with a median of approximately 1 to 1.3 μm, a very narrow span below 2 μm, and few outliers, reflecting its high repeatability and effective suppression of disturbance-induced spikes. The adaptive controller ranks second, with a median of approximately 2.7 to 3.0 μm and moderate variability, with a few runs exceeding 3.5 to 3.8 μm. This demonstrates the clear advantage of parameter learning, but its robustness is limited when unmodeled dynamics dominate. The SMC controller produces larger errors, with a median of approximately 3.5 to 4.0 microns and a wide range of fluctuations, consistent with residual tracking error caused by the boundary layer used to suppress chatter. The PID controller performed the worst, with a median of approximately 6.5 to 7.5 microns and the largest fluctuation range of 9 microns. The point distribution was relatively scattered, highlighting its susceptibility to parameter uncertainty and integral windup under disturbances. From a practical application perspective, ARC maintained the peak error below the critical 2-micron threshold in almost all cases, while the adaptive and SMC controllers frequently exceeded this level, and the PID controller almost always exceeded this level. In addition, ARC had the lowest coefficient of variation, indicating more stable performance during the experiment and reducing the need for readjustment. Overall, this distribution analysis confirmed that ARC not only achieved low steady-state errors, but also had excellent interference resistance and consistency, which are critical for maintaining surface quality, reducing mechanical stress, and ensuring strong process capabilities in precision applications.

7 Conclusion

This study proposes an adaptive robust micro-displacement control strategy and systematically validates its application in a rolling mill servo system. The core contribution of this research lies in bridging the gap between theoretical control design and the stringent requirements of high-precision industrial applications. By combining adaptive parameter estimation with robust compensation, the proposed controller effectively mitigates the dual challenges of parameter uncertainty and external disturbances inherent in large-scale rolling mill operation. Simulation and experimental results consistently demonstrate that tracking errors remain within 2 microns under a wide range of operating conditions, confirming not only the accuracy of the control law but also its robustness and repeatability. Compared with traditional PID, sliding mode, and purely adaptive schemes, the proposed approach achieves higher steady-state accuracy, stronger disturbance rejection, and more stable performance curves, highlighting its potential as a practical solution for industrial deployment. Beyond its direct applications, this study's contributions are threefold. First, it establishes a rigorous control framework that ensures microscale accuracy even in the presence of nonlinear dynamics and parameter drift, resolving a long-standing challenge in rolling mill automation. Second, it demonstrates the feasibility of embedding advanced adaptive robust strategies into practical servo systems, demonstrating that such approaches can transcend theoretical boundaries and be translated into engineering practice. Third, it provides a scalable foundation for future innovation: the control

concept can be extended to multi-axis coordinated motion, enabling precise synchronization of multiple mill stands, and its performance can be further enhanced by incorporating machine learning and predictive analytics for online parameter tuning and fault prediction. In summary, this paper not only provides a concrete control solution that outperforms traditional approaches in terms of accuracy and robustness, but also proposes a forward-looking framework that paves the way for intelligent, data-driven, and coordinated control strategies for the next generation of rolling mills.

8 Acknowledgement

Research on High Voltage Ultra Thin Current Collector Anti Breakage Strip Continuous High Speed Battery Pole Plate Rolling Mill Based on Advanced Control Technology (ZD24002). Study on the Design and Performance Optimization of Hollow-Core Fiber Devices Based on Hollow-Core Anti-Resonant Fibers (ZD25003).

References

[1] Y.-R. Liang, C.-Z. Zhao, H. Yuan, Y. Chen, W.-C. Zhang, J.-Q. Huang, D.-S. Yu, Y.-L. Liu, M.-M. Titirici, Y.-L. Chueh, H.-J. Yu, Q. Zhang, A review of rechargeable batteries for portable electronic devices, InfoMat 1(1)(2019) 6-32. https://doi.org/10.1002/inf2.12000

[2] J. Xiao, F.-F. Shi, T. Glossmann, C. Burnett, Z. Liu, From laboratory innovations to materials manufacturing for lithium-based batteries, Nature Energy 8(2023) 329-339. https://doi.org/10.1038/s41560-023-01221-y

[3] T. Günther, N. Billot, J. Schuster, J. Schnell, F.B. Spingler, H.A. Gasteiger, The Manufacturing of Electrodes: Key Process for the Future Success of Lithium-Ion Batteries, Advanced Materials Research 1140(2016) 304-311. https://doi.org/10.4028/www.scientific.net/AMR.1140.304

[4] Y.-J. Liu, S. Wang, J.-B. Qi, X.-W. Wang, X.-Q. Yan, Study on the Influence of Dynamic Characteristics of Servo Valve on Coupling Vibration of Cold Rolling Mill, International Journal of Precision Engineering and Manufacturing 25(8)(2024) 1557-1570. https://doi.org/10.1007/s12541-024-01017-4

[5] M. Chevalier, M. Gómez-Schiavon, A.-H. Ng, H. El-Samad, Design and Analysis of A Proportional-Integral-Derivative Controller with Biological Molecules, Cell Systems 9(4)(2019) 338-353. https://doi.org/10.1016/j.cels.2019.08.010

[6] H. Komurcugil, S. Biricik, S. Bayhan, Z. Zhang, Sliding Mode Control: Overview of Its Applications in Power Converters, IEEE Industrial Electronics Magazine 15(1)(2021) 40-49. https://doi.org/10.1109/MIE.2020.2986165

[7] I. Barkana, Simple Adaptive Control - A Stable Direct Model Reference Adaptive Control Methodology - Brief Survey, IFAC Proceedings Volumes 40(13)(2007) 310-327. https://doi.org/10.3182/20070829-3-RU-4911.00049

[8] C.-Y. Lin, T.L. Tseng, S.H. Emon, T.H. Tsai, Large Pre-Trained Models and Few-Shot Fine-Tuning for Virtual Metrology: A Framework for Uncertainty-Driven Adaptive Process Control in Semiconductor Manufacturing, IEEE Transactions on Automation Science and Engineering 22(2025) 15351-15370. https://doi.org/10.1109/TASE.2025.3568010

[9] F.-J. Lin, P.-H. Chou, C.-S. Chen, Y.-S. Lin, DSP-Based Cross-Coupled Synchronous Control for Dual Linear Motors Via Intelligent Complementary Sliding Mode Control, IEEE Transactions on Industrial Electronics 59(2)(2012) 1061-1073. https://doi.org/10.1109/TIE.2011.2157286

[10] P.-R. Jackson, T.-D. Wall, How Does Operator Control Enhance Performance of Advanced Manufacturing Technology?, Ergonomics 34(10)(1991) 1301-1311. https://doi.org/10.1080/00140139108964869

[11] Y. Zheng, A. Moreno, Y.-Q. Zhang, M.H. Sipponen, L. Dai, Harnessing chemical functionality of lignin towards stimuli-responsive materials, Trends in Chemistry 6(2)(2024) 62-78. https://doi.org/10.1016/j.trechm.2023.12.001

[12] S.-S. Chang, D. Yang, J.-Z. Cao, X. Li, An Extend Sliding Mode Disturbance Observer for Optical Inertial Platform Line-of–Sight Stabilized Control, Machines 12(12)(2024) 849.1-849.17. https://doi.org/10.3390/machines12120849

[13] E. Sariyildiz, K. Ohnishi, Stability and Robustness of Disturbance-Observer-Based Motion Control Systems, IEEE Transactions on Industrial Electronics 62(1)(2015) 414-422. https://doi.org/10.1109/TIE.2014.2327009

[14] J. Ogbemhe, K. Mpofu, N.-S. Tlale, Achieving Sustainability in Manufacturing Using Robotic Methodologies, Procedia Manufacturing 8(2017) 440-446.
https://doi.org/10.1016/j.promfg.2017.02.056
[15] Y. An, Y. Zeng, D. Luan, X.-W. Lou, Materials Design for High-Energy-Density Anode-Free Batteries, Matter 7(4) (2024) 1466-1502.
https://doi.org/10.1016/j.matt.2024.02.012
[16] F. Ubertini, I. Venanzi, G. Comanducci, Considerations on The Implementation and Modeling of An Active Mass Driver with Electric Torsional Servomotor, Mechanical Systems and Signal Processing 58-59(2015) 53-69.
https://doi.org/10.1016/j.ymssp.2014.12.010
[17] A.-C. Bertolino, M. Sorli, G. Jacazio, S. Mauro, Lumped Parameters Modelling of the EMAs' ball Screw Drive With Special Consideration to Ball/Grooves Interactions to Support Model-Based Health Monitoring, Mechanism and Machine Theory 137(2019) 188-210.
https://doi.org/10.1016/j.mechmachtheory.2019.03.022
[18] C. Meyer, H. Bockholt, W. Haselrieder, A. Kwade, Characterization of The Calendering Process for Compaction of Electrodes for Lithium-Ion Batteries, Journal of Materials Processing Technology 249(2017) 172-178.
https://doi.org/10.1016/j.jmatprotec.2017.05.031
[19] Y.-S. Liu, Robust Adaptive Observer for Nonlinear Systems with Unmodeled Dynamics, Automatica 45(8)(2009) 1891-1895.
https://doi.org/10.1016/j.automatica.2009.04.002
[20] E.-J. Bueno, A. Hernandez, F.-J. Rodriguez, C. Giron, R. Mateos, S. Cobreces, A DSP- and FPGA-Based Industrial Control with High-Speed Communication Interfaces for Grid Converters Applied to Distributed Power Generation Systems, IEEE Transactions on Industrial Electronics 56(3)(2009) 654-669.
https://doi.org/10.1109/TIE.2008.2007043
[21] O.-U. Lashmanov, A.-S. Vasilev, A.-V. Vasileva, A.-G. Anisimov, V.-V. Korotaev, High-Precision Absolute Linear Encoder Based on A Standard Calibrated Scale, Measurement 123(2018) 226-234.
https://doi.org/10.1016/j.measurement.2018.03.071